

基于 DSP—MCU 实现焊接电源系统数字化控制的设计

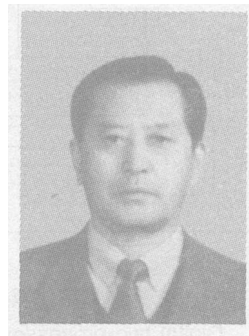
李鹤岐, 李春旭, 高忠林, 王 睿

(兰州理工大学 材料科学与工程学院, 甘肃省有色金属新材料国家重点实验室, 兰州 730050)

摘 要: 基于 DSP—MCU 实现焊接电源系统数字化控制的设计采用 TMS320F240 数字信号处理器和 80C196KC 单片机, 设计成实现多功能 IGBT 逆变焊接电源双机控制系统。其中, TMS320F240 主要用于焊接参数的采样、控制算法的运算, 80C196KC 用于完成人机接口的功能, 包括键盘和显示, 与上位机的通信等。设计中人机界面采用液晶显示。系统设计的关键是双机之间的通信技术, 为了确保通信的可靠及快速性采用双口 RAM (IDT7005) 来完成。数字 PWM 控制单元采用复杂可编程逻辑器件 (CPLD) 完成, 整个系统中所有逻辑控制也由此芯片来完成, 设计完成的 DSP—MCU 双机控制系统实现了焊机的多功能全数字化控制。

关键词: 脉宽调制; 复杂可编程逻辑器件; 数字信号处理器; 单片机; 数字化焊机

中图分类号: TG434 **文献标识码:** A **文章编号:** 0253—360X (2005)03—17—05



李鹤岐

0 序 言

数字化焊机是在逆变电源的基础上, 结合计算机技术, 采用数字信号处理器 (DSP), 通过微处理器的精确运算来控制焊机的各项性能及工作全过程, 控制电路高度集成、简化, 且实现了数控化。相对于采用以运算放大器、电阻、电容等为核心的控制系统, 不存在固有的元件参数漂移、性能随环境和时间而变化等缺点。所以, 焊接电源采用数字化控制, 有以下的主要优点: ①控制系统设计、开发的自由度大大提高。同样的硬件, 可以通过不同的软件来对焊机进行控制, 从而实现一机多用; ②系统的控制性能得到了很大的提高。模拟控制中固有的参数漂移等误差产生原因得以消除。不受模拟电路中补偿电路、滤波器等性能的制约, 容易得到理想的控制特性。使现代控制理论的应用及高级控制算法的实现成为可能; ③可靠性和易维修性得到了提高。无需对参数的漂移等进行调整和补偿, 系统的性能不受原器件特性的影响, 提高了系统性能的稳定性和抗干扰能力^[1]。该数字化逆变焊接电源系统的设计为全数字化焊接电源的研制奠定了基础。

1 数字化逆变双机系统设计

在控制系统设计中, 单片机本身的结构特点是控制功能较强, 而总线位数较少, 运行速度相对而言也要慢一些; 而 DSP 采用不同于单片机的结构, 其运算能力较强, 总线宽度也较宽, 而控制功能相对较弱。对于弧焊控制系统而言, 人机接口对速度要求较低, 而对控制能力的要求较高, 对总线宽度的要求较低, 一般 8 位就已经足够了。如果直接在 DSP 上扩展人机接口, 这样会浪费 DSP 芯片宝贵的外部控制能力。由于 DSP 经常需要响应慢速的人机接口中断, 这样对 DSP 的运算能力也是一个比较大的浪费。同时, 在现代生产中对焊接设备的实时性要求越来越高, DSP 强大的数据处理能力可以很好地满足这一要求。基于以上的考虑, 设计中采用将单片机和 DSP 合起来构成双机控制系统的方法, 以充分发挥单片机控制能力强的特点和 DSP 强大数据处理能力和高运行速度的优势。提高弧焊逆变电源控制系统的精度和实时性, 从而满足逆变弧焊机更高的性能要求。其系统框图如图 1 所示。

1.1 人机接口控制单元

设计中采用美国 INTEL 公司生产的 MCS96 系列 16 位单片机中的 80C196KC 作为人机接口控制单元。单片机主要完成人机接口的控制功能, 其中包括液晶显示、键盘面板以及与 PC (个人计算机)

收稿日期: 2004—04—23

基金项目: 甘肃省科技攻关项目 (GS035—A52—007—01); 甘肃省自然科学基金项目 (ZS032—B2500001)

* 参加该项目研究工作的还有路广

机的串行通信。

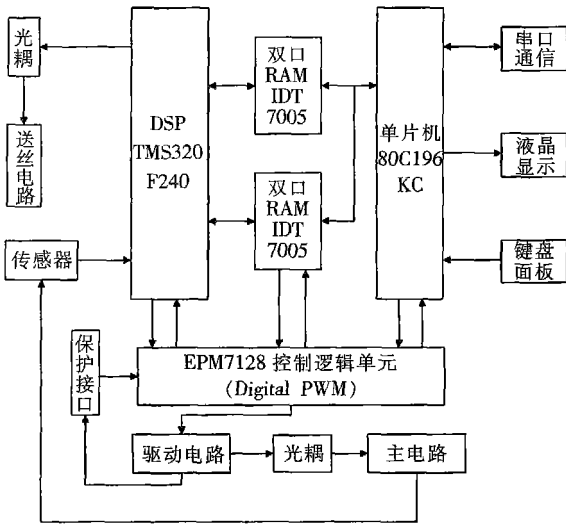


图 1 数字化双机控制系统框图

Fig 1 Digital two-processor controlling system diagram

1.2 键盘及液晶显示模块的设计

键盘包括“0—9”、“确认”、“上翻”、“下翻”、“取消”、“设置”共 16 个键位，通过 HD7279 与单片机相连。由于系统采用液晶模块对参数进行显示，故没有使用 HD7279 驱动数码管的功能。其原理图如图 2 所示。

采用图形点阵式液晶显示较之其它显示方式有以下优点：①工作电压低、功耗极低。工作电压 3~5 V，工作电流密度 $\leq 10 \mu A/cm^2$ ，特别适用于逆变电源显示。②液晶显示属被动显示，受外界光线干扰小。③图形点阵式液晶可显示的信息量大，分辨率高，不产生电磁干扰。④可靠性高，使用寿命长^[2]。

系统中所采用的液晶模块为 LG1601281-DW。对于液晶模块的控制一般有两种方法，直接法和间接法。设计中为了力求硬件线路的简单故采用直接法。其原理图如图 3 所示。

1.3 近程控制接口设计

研究试验中发现针对双机控制系统 RS-232

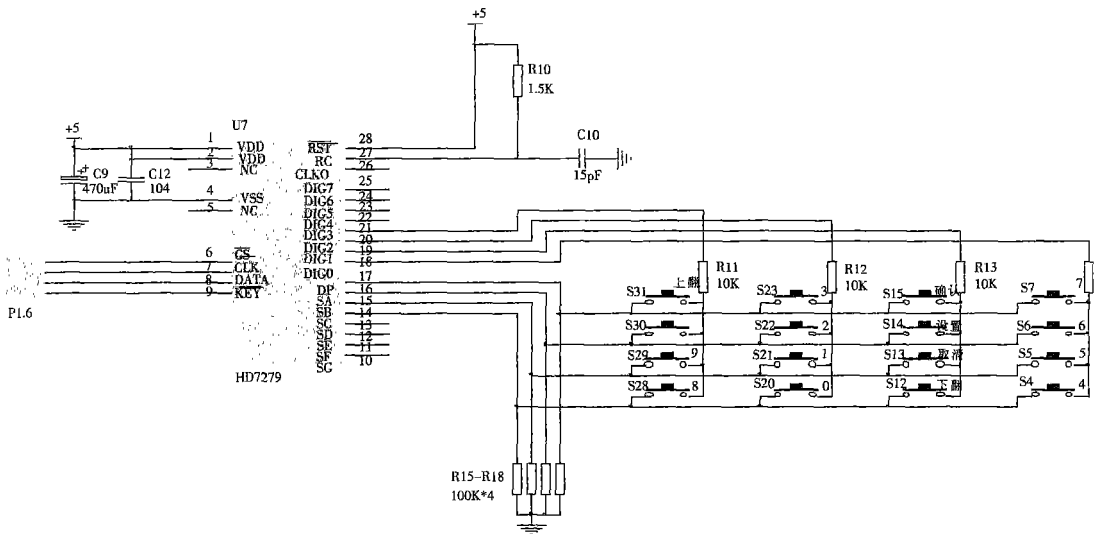


图 2 键盘原理图

Fig 2 Principle pbt of keyboard

接口有以下的缺点：①数据传输速率慢；②传送距离短；③未规定标准的连接器，因而出现了互不兼容的 25 芯连接器；④接口处各信号间容易产生串扰^[3]。鉴于此，设计采用 RS-485 接口来完成与上位机的通信。但一般在调试过程中，微机系统常用的是标准的 RS-232 接口，因此需要进行电平转换以实现两者互联；软件上，微机系统一般可采用简单灵活的 Visual Basic 编程，单片机则采用汇编语言。其硬件原理图如图 4 所示。

1.4 数字 P 控制单元

设计采用美国 TI 公司 TMS320F240 数字信号

处理芯片。该芯片采用 0.25 μm 的深亚微米 CMOS (互补金属氧化物半导体) 工艺制造，在单芯片上集成了具有高性能处理能力、低成本的 TMS320C2XX 核和经过优化的外设电路。典型的指令周期为 50 ns 可实时控制多种复杂控制算法。

设计中 DSP 主要用来完成数据的采集、A/D 转换、控制算法的运算。数字化弧焊逆变电源的输出电压、电流采样后经 A/D 转换送入 DSP，DSP 经计算后决定 PWM (脉宽调制) 的脉冲宽度并将其送至复杂可编程逻辑器件 (CPLD)。

1.5 数字 PWM 单元

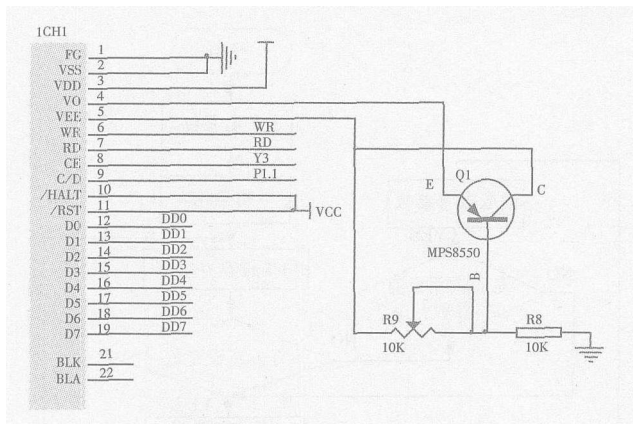


图 3 液晶显示原理图

Fig 3 Principle pbt for LCD display

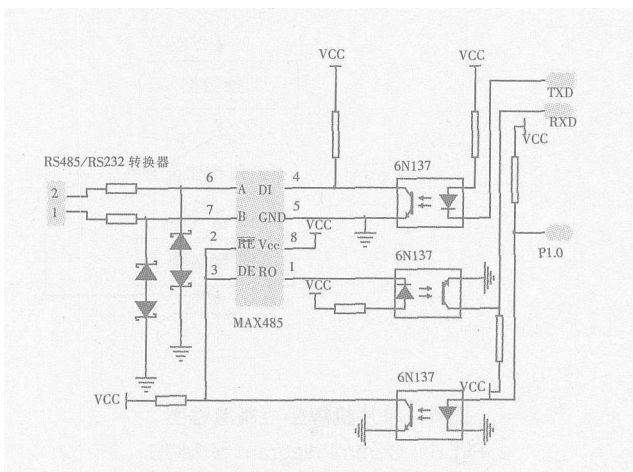


图 4 单片机与 PC 机通信原理图

Fig 4 Communication principle pbt between MCU and PC

在弧焊逆变电源中，数字化 PWM 芯片的设计是数字化弧焊逆变电源实现数字控制的关键。目前常用的 PWM 芯片在脉宽调制过程中通常要将数字量转换为模拟量，这样在转换过程中受转换芯片的精度以及干扰的影响，有时会降低整个系统控制精度及稳定性。鉴于此，系统设计中采用了复杂可编程控制器 CPLD 来完成数字 PWM 的功能。

复杂可编程逻辑器件属于专用集成电路 (ASIC) 的一种，其最大的特点是电路功能可以进行定制。与采用标准器件构成的设计相比 CPLD 有很大的灵活性。同时具有系统在线编程，高速传输信号，高可靠性，抗干扰能力强，功能强大，开发周期短等优点。

设计中采用 VHDL(超高速集成电路硬件描述语言)语言描述设计数字 PWM 芯片的电路结构和行为，用 Altera 公司的 MAX+PLUS II 将这些描述综合映射成与半导体工艺有关的硬件工艺文件，复

杂可编程器件作为这些硬件工艺文件的载体。当复杂可编程逻辑器件被加载，配置上相应的工艺文件后，进行器件烧结 (Programming)。所谓烧结就是将待烧结文件通过 JTAG 下载电缆配置到复杂可编程逻辑器件中。该复杂可编程逻辑器件便具有了相应的电路功能 [4]。

在此系统中基于计数器的 PWM 电路主要由四部分组成：(1) 装载电路：在计数器达到计数值 0 或终端计数值 M 时，载入占空比数据 DATA；(2) 计数电路：从 DATA 开始向下或向上计数，当计数器达到计数值 0 或终端计数值 M 后，产生装载脉冲电平；(3) 上下计数控制电路：当计数器载入数据或达到计数值“0”，“M”后，由装载脉冲电平控制计数器向下或向上计数；(4) PWM 输出电路：根据计数器输出信号的变化来产生 PWM 输出。当计数器载入数据 DATA 后，计数器开始向上计数，在此期间，PWM 输出为高电平；当计数器计数到终端值“M”再向上计数时，DATA 被重新载入，计数器开始向下计数，在此期间，PWM 输出为低电平；当计数到计数值“0”再向下计数时，新数据 DATA 被载入，PWM 开始了一个新的周期。为了对 IGBT(绝缘栅双基极晶体管)进行可靠的保护，CPLD 中还针对过流、过热以及过欠压等情况下封锁 PWM 脉冲输出的功能 [5]。

1.6 双机通信器件

在多处理器系统中，一般是以单片机作为主机，DSP 作为从机，后者主要完成系统的数字运算功能，而由单片机作为主机完成如通信，控制等功能，以及对从机进行复位，运行和挂起等控制。主机将从外部获得的给定数据交由从机处理。这样在主从式系统的设计中一个相当关键的问题就是两个处理器之间的数据交换 [3]。

目前应用比较多数据交换方案主要有以下几种：① 串行方式；② 并行方式；③ 分时总线方式；④ 双端口 RAM(随机存取存储器)方式。系统设计中若采用串行方式则效率过于偏低，而且会浪费 DSP 宝贵的运算时间，而 TMS320F240 不具备直接存储访问 (DMA) 功能，故不能采用分时总线方式。若采用并行方式则要占用大量的 I/O 口。而采用双端口 RAM 方式，其在数据通信时几乎不受干扰，实时性也极高，综合考虑各面的因素系统设计采用双端口 RAM 方式。

设计中采用的双端口 RAM 为 IDT7005。IDT7005 芯片是一种高速 8K 字节的 8 位双口静态随机存取存储器，其主要特性是：高速存取速度，最大存取时间有 20、25、35、55、70 ns 几种类型；低功

耗,工作状态耗电 550 mW (典型);可进行数据总线宽度扩展;可完成异步操作;片内端口的仲裁逻辑;TTL(晶体管-晶体管逻辑)电平,单电压 +5V, ±10%。试验表明该芯片完全满足数字化逆变电源控制系统双机通信的要求。

1.7 最优参数的储存

为了在系统中储存焊接专家参数,设计中采用了 X25045来完成此功能,同时通过此芯片来对单片机 80C196KC来复位。

X25045内部的存储器采用 CMOS工艺的 4096位串行 E²PROM(电可擦可编程只读存储器),按 512×8组织,每一字节可以擦写 10万次以上,内部数据可以保存 100年以上。芯片具有可编程块锁定功能。使用三线总线的串行外设接口对 X25045进行读写操作。

1.8 送丝系统

在焊接过程中,DSP检测焊枪开关的状态来决定是否给出送丝与送气的启/停信号及送丝速度的给定值。送丝控制系统采用 PWM控制的 DC-DC斩波电路。利用 DSP的 PWM输出口输出 PWM信号。通过调节 PWM信号的占空比来改变 MOSFET(金属氧化物半导体场效应晶体管)的导通时间,从而达到改变送丝速度的目的。

2 控制系统软件结构

设计中系统软件采用模块化设计方案,包括采用单片机汇编语言编写的焊接控制程序、采用 DSP汇编语言编写的数据处理程序以及采用 VHDL语言编写的数字 PWM程序。其流程图如图 5、图 6、图 7所示。

3 结 论

数字化多功能逆变焊机双机控制系统的工作过程:操作者首先通过控制面板设置焊接参数或者调用储存在系统中的最优参数,主机通过双口 RAM将参数送给 DSP,焊接过程开始。在焊接过程中实际焊接参数经采样后在 DSP中通过控制算法得到控制量。同时,采样后的参数也将通过双口 RAM回送给单片机,用于液晶模块的实时显示。DSP通过控制算法所得到的控制量被送给 CPLD后,由其产生驱动 IGBT的两路脉冲。整个过程由于都是数字信号的传输和比较,因此,非常迅速、精确和抗干扰。通过运用 DSP等高性能处理器,使采用复杂的

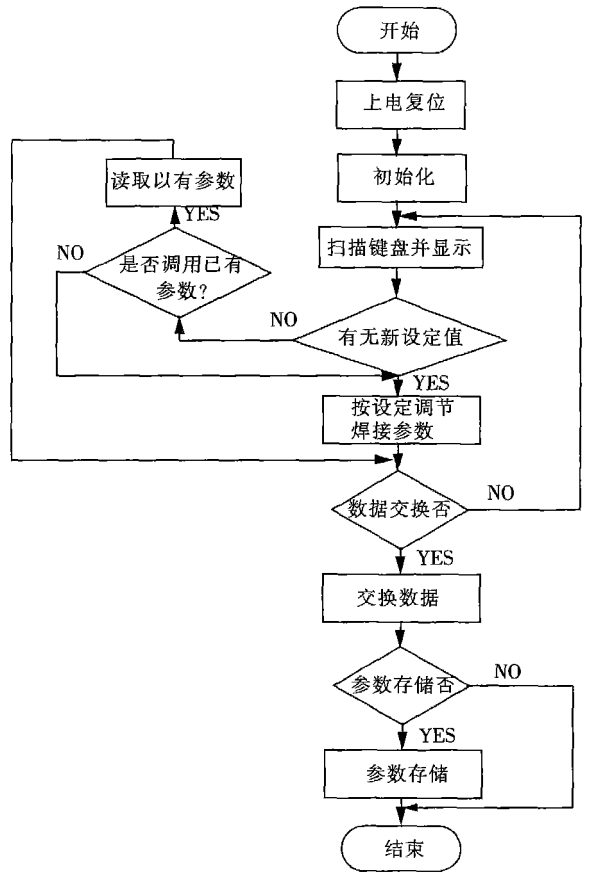


图 5 单片机焊接控制流程图

Fig. 5 Control diagram of MCU

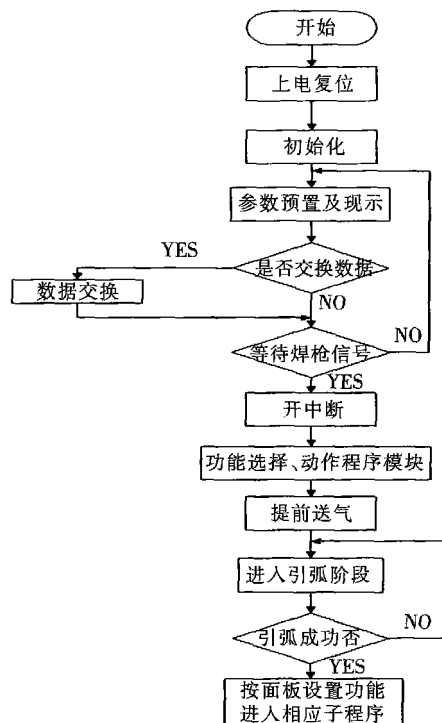


图 6 DSP工作流程图

Fig. 6 Control diagram of DSP

表 1 复合热源缝焊缝抗剪强度

Table 1 Shearing strength of lap joints by laser-TIG hybrid welding

焊接速度 $v/(mm \cdot min^{-1})$	抗剪强度 τ /MPa	母材百分比 %
900	193.3	80.1
1000	164.9	68.3
1100	149.8	62.1
1200	111.5	46.2

4 结 论

(1) 采用激光-TIG复合热源缝焊镁合金能够得到质量良好的焊缝并且焊接工艺参数范围较宽。

(2) 缝焊缝熔深是评定焊接质量的重要依据,熔深越大两层间的结合愈牢固。焊接速度、激光

斑点与电弧中心距离、离焦量对缝焊熔深均有很大影响。

(3) 激光-TIG复合热源缝焊镁合金可以得到抗剪强度较高的焊接接头,是一种优良的焊接工艺。

参考文献:

- [1] 彭毅, 郑大春. 激光加工在汽车工业生产中的应用[J]. 新材料新工艺, 2000, (7): 15-17.
- [2] Moriaki Ono, Yukio Shinbo, Akihide Yoshitake. Development of laser arc hybrid welding[J]. NKK Technical Review, 2002, 86: 8-12.

作者简介: 迟鸣声, 男, 1980年7月出生, 硕士研究生。主要研究方向为镁合金复合热源焊接工艺及其数值模拟。

Email: liuhm@dlut.edu.cn

[上接第 20 页]

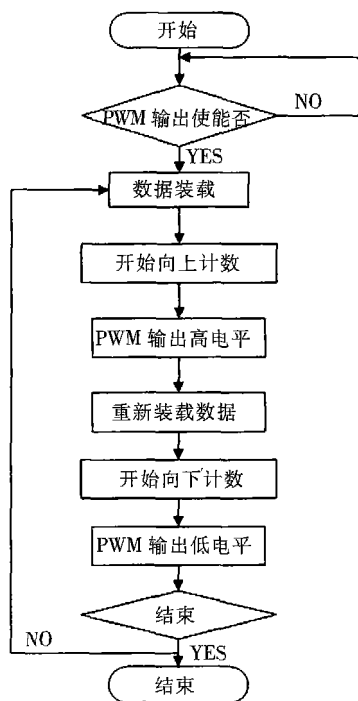


图 7 数字 PWM 流程图

Fig. 7 Digital PWM diagram of CPLD

控制算法成为可能。焊机采用键盘输入及液晶显示,从而使参数预置和显示实时、清晰明了。DSP-MCU双机通信采用双口RAM使通信的速度以及

抗干扰能力得到极大的提高。X25045的运用使焊机具有了储存最优参数的能力,方便操作者使用。同时,运用CPLD来产生PWM信号,可以弥补通用PWM的不足,通过VHDL语言来自行设计具有PWM功能的芯片,使系统的整体性能得到了加强。试验结果证明所设计的控制系统完全满足多功能数字化逆变焊机控制要求。

参考文献:

- [1] Liu Jia, Lu Zheng yang Yin Shuyan. The digitalization of welding inverter[J]. Transactions of the China Welding Institution, 2002, 23(1): 88-92.
- [2] 刘嘉, 卢振洋, 殷树言, 等. 电焊机的数字化[J]. 焊接学报, 2002, 23(1): 88-92.
- [3] 公茂法, 马宝甫, 孙晨. 单片机人机接口实例集[M]. 北京: 北京航空航天大学出版社, 1998. 63-65.
- [4] 李朝青. PC机及单片机数据通信技术[M]. 北京: 北京航空航天大学出版社, 2000. 103-114.
- [5] 宋万杰, 罗丰, 吴顺君. CPLD技术及其应用[M]. 西安: 西安电子科技大学出版社, 1999. 83-107.
- [6] 程杰斌, 王华民, 李劲松, 等. 基于CPLD的全数字脉宽调制器的设计[J]. 电力电子技术, 2003, 37(3): 76-78.

作者简介: 李鹤岐, 男, 1940年5月出生, 教授, 博士生导师。主要研究方向为材料加工过程智能控制与自动化。获省部级科技成果奖7项,发表研究论文80余篇。

Email: lihq@lut.cn

MAIN TOPICS, ABSTRACTS & KEY WORDS

Two-dimensional flow of plasticized materials in friction stir welded joints KE Li-ming XING Li HUANG Feng-an (School of Material Science and Engineering Nanchang Institute of Aeronautical Technology Nanchang 330034, China). p1-4

Abstract The two-dimensional flow behavior of the plasticized materials in friction stir welded joints of aluminum LF6 was investigated with the copper sheet as an insert tracer material. The distribution of the copper on the plane parallel to the surface was observed by optical microscopy. The results indicate that the material flow was asymmetrical on the plane parallel to surface during friction stir welding. On the advancing side, the material in the parent metal flowed along the welding direction and the material in the weld flowed opposite to the welding direction; on the retreating side, the material only flowed opposite to the welding direction and some flowed into advancing side behind the pin. To analyze the material flow pattern on the plane parallel to the surface, a tentative two-dimensional extrusion mode was presented based on the assumption that there was a thermal plasticized zone close to the pin. During welding, the shape of the zone was steady if the center of the pin was taken as the original point of the coordinate. The effect of the pin's rotational and linear movement on the plasticized material within the thermal plasticized zone was analyzed separately and the flow pattern could be given according to these movements, which could explain the distribution of the tracer material observed.

Key words friction stir welding; tracer material; extrusion mode; aluminum

Depositing light ceramic coating on high temperature polymer matrix composite substrate ZHANG Yan-liang^{1,2}, GUO Mian-Huan¹, LIU Ai-guo¹, ZHAO Min-hai¹ (1. National Key Laboratory of Advanced Welding Production Technology Harbin Institute of Technology Harbin 150001, China; 2. Wendeng Cutting Tool Factory Wendeng 264000, Shandong China). p5-8

Abstract Feasibility of depositing Al_2O_3 coating on carbon fiber reinforced polymer matrix composite (PMC) with Ni-3% Al powder, aluminum or zinc as the bond layer was investigated. Shear strength and thermal cycling resistance of the coatings were tested. The results showed that plasma sprayed Ni-3% Al powder would damage the PMC substrate and was not suitable for bonding ceramic coating on PMC substrate. Arc sprayed aluminum would make some damage to the substrate, too. And the shear strength and thermal cycling resistance of the coating were low. Arc sprayed zinc with low voltage and low current would form good bond layer on PMC substrate, and the shear strength could be as high as 10.45MPa. Thermal cycling resistance of Al_2O_3 coating deposited on zinc bond layer was good.

Key words high temperature polymer matrix composite; ceramic coating; spray; bond layer

Impact wear-resistant hardfacing austenitic material LIU Zheng-jun, LIU Chen, CHEN Hong, LI Yong-kui, CHENG Jiang-bo, SU Yun-hai, LIU Duo (Department of Material Sciences and Engineering, Shenyang University of Technology, Shenyang 110023, China). p9-12

Abstract One kind of hardfacing austenitic electrode for impact wear-resistance, named EKCM50, which is a Fe-Mn-Cr-Mo-V alloy system, was developed. Experiments and analysis show that the wear-resistance properties of the deposited metal are higher than that of the D256 electrode. After work-hardening impact experiments, the hardness of EKCM50 bead weld layer increases from 32HRC to 45HRC. After 40 min of impact wear experiments, the weight loss of deposited metal is very slight. The mechanism of strain-hardening and wear-resistance of welding material and the influence of these alloying elements on wear-resistance was discussed.

Key words impact wear; hardfacing; work-hardening

Microstructure characteristics of induction brazed TiAl/35CrMo joint with Ag-Cu-Ni-Li filler metal XU Wei, HE Jing-shan, FENG Ji-cai (National Key Laboratory of Advanced Welding Production Technology Harbin Institute of Technology Harbin 150001, China). p13-16

Abstract Microstructure of the induction brazed TiAl/Ag-Cu-Ni-Li/35CrMo joints was analyzed by means of scanning electron microscope, electron probe microanalysis and energy dispersive X-ray spectrometry. The results show that there is a wide reaction zone and narrow reaction zone in the brazed seam along radial orientation of the brazed joints. The two zones are situated outside and inside of the brazing seam respectively. The boundary of two zones is obvious. The interface structure of the joint brazed at 900°C for 5 min can be expressed as TiAl/diffusion layer between TiAl and brazing filler metal/Ag-rich, Cu-rich phase /Ti(Cu, Al)₂/Ag-rich phase /AM₂Ti (M represents Fe, Cu, Ni) / the diffusion layer between brazing filler metal and 35CrMo / 35CrMo. The morphoses of the reaction layer near TiAl side is equiaxial crystal and columnar crystal of Ti(Cu, Al)₂. There exists orientation relationship between Ti(Cu, Al)₂ and TiAl.

Key words induction brazing; microstructure characteristics; Ag-Cu-Ni-Li filler metal; TiAl

Investigation of digital controlling in welding power system based on DSP and MCU LI He-qi, LI Chun-xu, GAO Zhong-lin, WANG Rui, LU Guang (Education Ministry Key Lab. of Advanced Processing

Technology for Non-ferrous Materials Lanzhou University of Technology
Lanzhou 730050, China). p17-20, 24

Abstract A two-processing controlling digital inverter welding power system was designed based on digital signal processor(DSP) and micro-control unit(MCU) and its multi-functions were achieved. DSP (TMS320F240) was mainly used in sampling welding parameters and calculating control algorithm, whereas MCU (80C196KC) was used in implementing interfaces including keyboard, display and communication. Liquid crystal display is adopted for man-machine interaction. The key point of the design was the communication between DSP and MCU, therefore a dual port RAM (IDT7005) was adopted to ensure its reliability and rapidity. Complex programmable logic device was used to realize digital pulsed width modulation. The results indicates that fully digital controlling of multi-function welding machine was realized through DSP/MCU controlling system.

Key words pulsed width modulation; complex programmable logic device; digital signal processing; micro-control unit; digital welding power

Laser-TIG hybrid overlap welding process of AZ31B Mg alloy
CHIMing-Sheng, LIU Li-Ming, SONG Gang (State Key Laboratory of Material Surface Modification by Laser, Ion- and Electronic beams
Dalian University of Technology, Dalian 116024, China). p21-24

Abstract Wrought magnesium alloy AZ31B was welded with laser-TIG (tungsten inert-gas) hybrid overlap welding process and the surface appearance of the bead, the influencing factors of the penetration and shear strength were discussed. The results show that the bead evidently presents "pin shape" when welded by laser-TIG hybrid overlap welding. The top of bead is the typical shape when welded with TIG process, while the bottom of bead showed the typical shape of laser welding. It was a good way to weld magnesium alloy by using the laser-TIG hybrid welding with advantages high welding speed, aesthetic bead form, comparative wide welding parameters and high shear strength of joints.

Key words AZ31B Magnesium alloy; hybrid overlap welding; shear strength; laser-tungsten inert-gas welding

Numerical model of heat input from rotational tool during friction-stir welding
WANG Da-yong, FENG Ji-cai, WANG Pan-feng (National Key Laboratory of Advanced Welding Production Technology, Harbin Institute of Technology, Harbin 150001, China). p25-28, 32

Abstract This paper has established the numerical models of the heat generation from the shoulder, the cylinder-shape and the cone-shape pins (including pin sideface and endface) during friction-stir welding. The effect of pin angle on the heat generation from the cone-shape pin has been analyzed. The results confirm that the heat generation from the shoulder and the cone-shape pin endface decreases, and the heat generation from the cone-shape pin sideface increases when pin angle increases. However, the general heat generation from the cone-shape pin decreases firstly, then increases rapidly, with pin angle increasing.

Key words friction-stir welding; heat input; numerical model

Effect of trace Zr on microstructures and properties of welded joint of Al-5.8Cu-0.3Mn alloy
LI Hui-zhong, ZHANG Xin-ming, CHEN Ming-an, LIU Ying, ZHOU Zhuo-ping (School of Materials Science and Engineering, Central South University, Changsha 410083, China). p29-32

Abstract Al-5.8Cu-0.3Mn alloy was welded using 4047 solder wire with metal inert-gas welding. Mechanical properties and microstructures of the welded joints and base metals were studied by means of optical microscope, transmission electron microscope and microhardness. The experimental results show that the tensile strength of base metal can be improved by 30 MPa and the tensile strength of the welded joint can be improved by 50 MPa. At the same time, the microstructures of recrystallization of the welded zone are fined due to addition of 0.21% Zr. The tensile strength of the welded joint of Al-5.8Cu-0.3Mn alloy is lower than that of the base metal. In the welded joint the weld bead is the weakest area and the soften zone in the heat affected zone is the second weakest where the θ' phase particle became coarser.

Key words Al-5.8Cu-0.3Mn alloy; welded joint; microstructure; tensile strength properties

Influence of coaxial shielding gas flux on keyhole in Nd:YAG CW laser deep-penetration welding
QIN Guo-liang, Lin Shang-yang (Harbin Welding Institute, Harbin 150080, China). p33-36

Abstract The influence of coaxial shielding gas flux on keyhole was studied by processing the captured coaxial image of keyhole. The results show that the coaxial shielding gas has great influence on the upside of keyhole and its influence on keyhole bottom is weak. For more flux of coaxial shielding gas, the radial dimension of outer edge of keyhole increases but the radial dimension of inner edge of keyhole varies little. The distances from the centers of keyhole edges to that of laser spot decrease with increasing the flux of coaxial shielding gas, which indicates that the vertical axis of keyhole is nearer to that of laser beam. In general, coaxial shielding gas has little influence on keyhole.

Key words solid laser; deep-penetration welding; keyhole; coaxial shielding gas; flux

Morphology processing image of aluminum alloy metal inert-gas welding pool
SHI Yu^{1,2}, FAN Ding^{1,2}, WU Wei¹ (1. State Key Lab of Advanced Non-ferrous Materials, Lanzhou University of Technology, Gansu Province, Lanzhou 730050, China; 2. Education Ministry Key Lab of Advanced Processing Technology for Non-ferrous Materials, Lanzhou 730050, China). p37-40

Abstract Weld pool geometry is a crucial factor in determining welding quality and its feedback control is a fundamental requirement of automated welding. Therefore, a vision sensing system for taking and processing the image of metal inert-gas(MIG) welding pool of aluminum alloy is developed. Clear images of the MIG welding pool are obtained by u-